

# Computation of 2D vibroacoustic wave's dispersion for optimizing acoustic power flow in interaction with adaptive metamaterials

M. Collet<sup>a</sup>, M. Ouisse<sup>a</sup>, M. Ichchou<sup>b</sup> and R. Ohayon<sup>c</sup>

<sup>a</sup>Dept Applied Mechanics, FEMTO-ST UMR 6174, 24 chemin de l'Épitaphe, 25 000 Besançon, France;

<sup>b</sup>LTDS, CNRS UMR5513, Ecole Centrale de Lyon, 36 av Guy de Collongue, 69134 Ecully, France;

<sup>c</sup>3LMSSC, EA3196, CNAM, 2 rue Cont, 75141 Paris.

## ABSTRACT

This paper presents an integrated methodology for optimizing vibroacoustic energy flow in interaction between an adaptive metamaterial made of periodically distributed shunted piezoelectric material glued onto passive plate and open acoustic domain. The computation of interacting Floquet-Block propagators is also used to optimize vibroacoustic. The main purpose of this work is first to propose the numerical methodology to compute the fluid-structure multi-modal wave dispersions. In a second step optimization of electric circuit is used to control the acoustic power flow. 3D standard computation is used to confirm the efficiency of the designed metamaterial in term of acoustic emissivity and absorption.

**Keywords:** Distributed control, 2D Waves Dispersion, Bloch Theorem, Shunted piezoelectric, Mid-Frequency Optimization

## 1. INTRODUCTION

Tailoring the dynamical behavior of wave-guide structures can provide an efficient and physically elegant approach for optimizing mechanical components with regards to vibration and acoustic criteria, among others. However, achieving this objective may lead to different outcomes depending on the context of the optimization. In the preliminary stages of a product's development, one mainly needs optimization tools capable of rapidly providing global design directions. Such optimization will also depend on the frequency range of interest. Thus, piezoelectric materials and other adaptive and smart systems are employed to improve the vibroacoustic quality of structural components, especially in the Low Frequency range<sup>1-3</sup> even if distributed transducers are used.<sup>4</sup> Recently, much effort has been spent on developing new multi-functional structures integrating electro-mechanical systems in order to optimize their vibroacoustic behavior over a larger frequency band of interest.<sup>5-13</sup> For Medium Frequency band some specific approaches have been developed known as metamaterial concept firstly introduced in.<sup>14,15</sup> This concept couples two different aspects in vibration control. The first concept is connected to periodic structures theories usually connected to metamaterial developments. In this case, it is well known that the dynamic behavior is fully connected to periodicity ratios and existing pass bands and blocked bands can be of real use in vibration control. The second concept is associated to vibration control through piezoelectric and smart materials. Specifically, shunted piezoelectric smart materials are employed for the metamaterial achievement by integrating into the metamaterial electronics and numerical components allowing implementation of adaptive and controlled behavior. We also tend to extend the notion of programmable matter within the meaning of work presented in<sup>16</sup> to vibroacoustic programming. First application of this concepts has been already done for controlling mechanical energy power flow in<sup>15</sup> or by processing acoustic radiation effect in.<sup>17</sup>

In this paper, we present an integrated methodology for optimizing vibroacoustic energy flow in interaction between an adaptive metamaterial made of periodically distributed shunted piezoelectric material glued onto

---

Further author information: (Send correspondence to M. Collet)

M. Collet: E-mail: manuel.collet@univ-fcomte.fr, Telephone: 3 381 666 728

passive plate and open acoustic domain. Extension of shifted cell operator methodology to fluid-structure interaction is presented. The computation of interacting Floquet-Bloch propagators is also used to optimize vibroacoustic indicators as noise absorption and emission. The main purpose of this work is first to propose the numerical methodology to compute the fluid-structure multi-modal wave dispersions. In a second step optimization of electric circuit is used to control the acoustic power flow.

After recalling the Floquet-Bloch theorems, we introduce a new numerical formulation for computing the multi-modal damped wave numbers dispersion in the whole first Brillouin domain of a periodical smart structure made of periodically distributed shunted piezoelectric patches. Based on this wave modeling, optimization of the electrical impedance of the shunted circuit is made in order to decrease group velocity of flexural waves. The obtained optimal impedance is also tested in controlling the HF response of a semi-distributed system.

## 2. APPLICATION OF THE FLOQUET-BLOCH THEOREM TO MODEL ADAPTIVE FLUID STRUCTURE INTERACTIONS

In this section the application of the Floquet-Bloch theorem is presented for piezo-elastodynamic and acoustic interaction problem. Based on the well known results obtained by Floquet<sup>18</sup> in one-dimensional and later rediscovered by Bloch<sup>19</sup> in multidimensional problems, we propose an original application to bi-dimensional piezo-elastodynamical and acoustic problem leading to very general numerical implementation for computing waves dispersion for periodically smart distributed mechanical systems incorporating electronic components and damping effects.<sup>14, 15, 20</sup>

### 2.1 The shift cell operator for fluid-structure interaction problem

Application to the Floquet-Bloch theorem for computing complex waves dispersion in piezo-elastodynamical problem via the resolution of the shift cell operator eigensolutions is described in.<sup>14, 15</sup> In this paper we consider a fluid-structure periodic system made of unitary cells as depicted in figure . It is made of a supporting aluminum plate on which a circular piezoelectric patch is glued. On the other plate face, we consider an acoustic parallelepiped domain bounded by a rigid wall far from the elastic plate. All dimensions are presented on figure . The fluid structure interaction is written by imposing continuity of the normal velocity and acoustic pressure is applied on the structural domain.

The shift cell operator, its weak formulation for computing waves dispersion into periodical piezocomposite lattice is precisely described in.<sup>15</sup> We also just introduce here the acoustic application of the previously described methodology. The Helmholtz equation governing the acoustic equilibrium and its corresponding boundary conditions are given by :

$$\frac{\omega^2}{C_o^2}p(\mathbf{x}) + \nabla^2 p(\mathbf{x}) = 0 \quad \forall \mathbf{x} \in \Omega_f \quad (1)$$

$$p(\mathbf{x})_{\Gamma_{x-}} = p(\mathbf{x})_{\Gamma_{x+}} \quad (2)$$

$$p(\mathbf{x})_{\Gamma_{y-}} = p(\mathbf{x})_{\Gamma_{y+}} \quad (3)$$

$$\mathbf{n} \nabla p(\mathbf{x}) = 0 \quad \forall \mathbf{x} \in \Gamma_\infty \quad (4)$$

$$\mathbf{n} \nabla p(\mathbf{x}) = -\omega^2 \rho_o \mathbf{n} \cdot \mathbf{w}(\mathbf{x}) \quad \forall \mathbf{x} \in \Gamma_\S \quad (5)$$

where  $\omega$  is the angular frequency,  $C_o$  the speed of sound in the medium,  $\rho_o$  the fluid mass density,  $\mathbf{n}$  the unitary normal vector,  $\mathbf{w}$  the plate displacement. The first boundary condition 4 represent the hard wall condition, the last one, in equation 5, is the fluid structure interaction condition corresponding to the continuity of the normal displacements. We note that the adjoint condition is applied by imposing acoustic pressure acting on the mechanical structure. The continuity conditions on lateral faces  $\Gamma_{x-}$ ,  $\Gamma_{x+}$ ,  $\Gamma_{y-}$  and  $\Gamma_{y+}$  of the primitive cell of the periodic problem are directly linked to the use of the Floquet-Bloch theorem for computing of the Bloch eigenmodes and the associated dispersion curves. The main idea is to search the generalized eigenvalue problem given by equations (1),(4), (5) when the pressure  $p(\mathbf{x})$  (and also displacement and voltage) can be written as :

$$p(\mathbf{x}) = p_{n,k}(\mathbf{x}) e^{i\mathbf{k} \cdot \mathbf{x}} \quad (6)$$

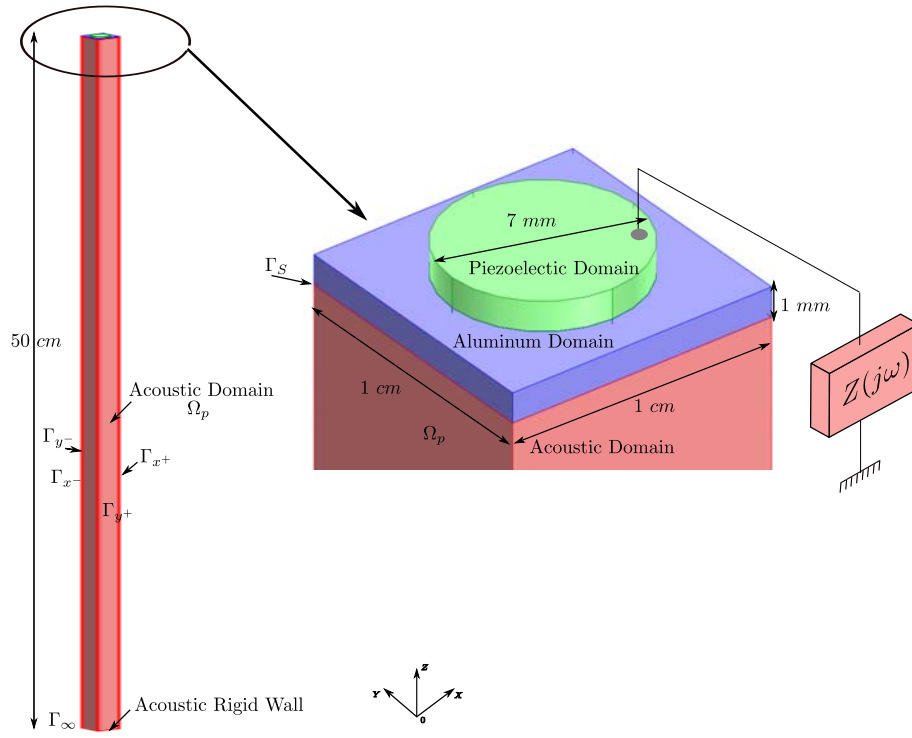


Figure 1. Generic 3D piezocomposite periodic cell

with  $p_{n,k}(\mathbf{x})$ ,  $\Omega_f$  periodic functions (i.e  $p_{n,k}(\mathbf{x})_{\Gamma_{x^-}} = p_{n,k}(\mathbf{x})_{\Gamma_{x^+}}$  and  $p_{n,k}(\mathbf{x})_{\Gamma_{y^-}} = p_{n,k}(\mathbf{x})_{\Gamma_{y^+}}$ ). By introducing expression (6) in the acoustic equations (1), one can demonstrate that  $p_{n,k}(\mathbf{x})$  and  $\omega_n(\mathbf{k})$  are solutions of the generalized eigenvalues problem:

$$\left(\frac{\omega^2}{C_o^2} - \mathbf{k}^2\right)p_{n,k}(\mathbf{x}) + 2i\mathbf{k}\nabla p_{n,k}(\mathbf{x}) + \nabla^2 p_{n,k}(\mathbf{x}) = 0 \quad (7)$$

with the associated boundary conditions :

$$\begin{cases} p_{n,k}(\mathbf{x})_{\Gamma_{x^-}} = p_{n,k}(\mathbf{x})_{\Gamma_{x^+}} \\ p_{n,k}(\mathbf{x})_{\Gamma_{y^-}} = p_{n,k}(\mathbf{x})_{\Gamma_{y^+}} \\ \mathbf{n}(\nabla p_{n,k}(\mathbf{x}) + i\mathbf{k}p_{n,k}(\mathbf{x})) = 0 & \forall \mathbf{x} \in \Gamma_\infty \\ \mathbf{n}(\nabla p_{n,k}(\mathbf{x}) + i\mathbf{k}p_{n,k}(\mathbf{x})) = -\omega^2 \rho_o \mathbf{n} \cdot \mathbf{w}_{n,k}(\mathbf{x}) & \forall \mathbf{x} \in \Gamma_\S \end{cases} \quad (8)$$

where  $\mathbf{k} = k \begin{bmatrix} \cos(\phi) \\ \sin(\phi) \\ 0 \end{bmatrix} = k\Phi$  where  $\phi$  represent the direction angles into the reciprocal 2D lattice domain.

These acoustic equations are associated with the piezoelastodynamical one presented in.<sup>14</sup>

The proposed formulation is also based on the computation of the Floquet vectors (equation (7)), instead of computing the Floquet propagators commonly used for elastodynamic applications. Our approach allows to obtain the full 2D waves dispersions functions and to clearly introduce damping and electrical impedance into the acousto-piezo-elastodynamic operator. The adopted methodology allows the computation of the complete complex map of the dispersion curves incorporating computation of evanescent waves and allowing the introduction of damping and shunt operator if any.

## 2.2 Numerical Computation of the Bloch's waves

The numerical implementation is obtained by using a standard finite elements method to discretize the adapted weak formulation as specified in.<sup>14</sup> The assembled matrix equation is given by:

$$(K(Z(i\omega_n(\lambda, \phi)) + \lambda L(\phi, Z(i\omega_n(\lambda, \phi))) - \lambda^2 H(\phi, Z(i\omega_n(\lambda, \phi))) - \omega_n^2(\lambda, \phi)M)u_{n,k}(\phi) = 0, \quad (9)$$

where  $\mathbf{u}_{n,k}(\phi)$  represents the extended degrees of freedom vector made of displacements  $\mathbf{w}$ , voltage  $V$  and pressure  $p$ ,  $\lambda = ik$ ,  $M$  and  $K(Z(i\omega_n(\lambda, \phi)))$  are respectively the standard symmetric semi-definite mass and stiffness matrices (the mass matrix is semi definite because elastostatic equation are condensed into the equation),  $L(\phi, Z(i\omega_n(\lambda, \phi)))$  is a skew-symmetric matrix and  $H(\phi, Z(i\omega_n(\lambda, \phi)))$  is a symmetric semi-definite positive matrix.

When  $k$  and  $\phi$  are fixed and  $Z$  does not depend on  $\omega$  the system (9) is a linear eigen value problem allowing us to compute the dispersion functions  $\omega_n^2(\mathbf{k}, \phi)$  and the associated Bloch eigenvector  $\mathbf{u}_{n,k}(\phi)$ .

This approach has been widely used for developing homogenization techniques and spectral asymptotic analysis like in the work of.<sup>21</sup> It can also be applied for computing wave's dispersion even if Floquet propagators is preferred for 1D or quasi 1D computation, as indicated in.<sup>22-24</sup> Nevertheless these approaches have been only developed for undamped mechanical systems that is to say represented by a set of real matrices. In this case, most of the previously published works present techniques based on the mesh of a real  $\mathbf{k}$ -space (i.e  $\mathbf{k}$  or  $\lambda$  and  $\phi$ ) inside the first Brillouin zone for obtaining the corresponding frequency dispersion and the associated Floquet vectors. For undamped system only propagative or evanescent waves exist corresponding to a family of eigen solutions purely real or imaginary. Discrimination between each class of waves is easy. If a damped system is considered ( $K, L, H$  are complex frequency dependent) or frequency dependence of the electrical shunt impedance is considered, the obtained eigenvalue problem is not quadratic and a complex specific numerical methodology has to be implemented. Furthermore, evanescent part of propagating waves appear as the imaginary part of  $\omega_n^2(\lambda, \Phi)$ . It then becomes very difficult to distinguish the propagative and evanescent waves but also to compute the corresponding physical wave's movements by applying spatial deconvolution.

Another much more suitable possibility for computing damped system, dedicated for time/space deconvolution and for computation of diffusion properties as defined by,<sup>5,24</sup> is to consider the following generalized eigen value problem:

$$(K(Z(\omega) - \omega^2 M + \lambda_n(\omega, \phi)L(\phi, Z(\omega)) - \lambda_n^2(\omega, \phi)H(\phi, Z(\omega)))u_n(\omega, \phi) = 0. \quad (10)$$

In this problem, the pulsation  $\omega$  is a real parameter corresponding to the harmonic frequency. Wave's numbers and Floquet vectors are then computed. An inverse Fourier transformation in the  $k$ -space domain can lead us to evaluate the physical wave's displacements and energy diffusion operator when the periodic distribution is connected to another system as in.<sup>5</sup> Another temporal inverse Fourier transformation can furnish a way to access spatio-temporal response for non-homogeneous initial conditions. As  $L$  is skew-symmetric, the obtained eigen values are quadruple  $(\lambda, \bar{\lambda}, -\lambda, -\bar{\lambda})$  collapsing into real or imaginary pairs (or a single zero) when all matrices are real (i.e. for an undamped system). In this case a real pair of eigen values correspond to evanescent modes oriented in two opposite directions on the  $k$ -space and imaginary values to two traveling waves propagating in opposite direction.

As previously mentioned, the real part of  $\mathbf{k} = k\Phi$  vector is restricted to stand inside the first Brillouin zone. In the quadratic eigen value problem (10) nothing restricts computation to only find eigen values satisfying this condition. For direction vector  $\Phi$  orthogonal to the lattice facelets (i.e. for  $\Phi_{p1} = [1, 0]^T$  and  $\Phi_{p2} = [0, 1]^T$  in bi-dimensional rectangular cell), the periodical conditions expressed for one dimensional wave guide are still valid: if  $\lambda_j(\omega, \Phi_p)$  is an eigen value associated to  $\mathbf{w}_j(\omega, \Phi_p)$  then  $\forall \mathbf{m} \in \mathbb{Z}^3$ ,  $\lambda + i \cdot \Phi_p^T(G \cdot \mathbf{m})$  is also an eigen value associated to  $\mathbf{w}_j(\omega, \Phi_p)e^{-i \cdot \Phi_p^T(G \cdot \mathbf{m})x}$ . Thus, for undamped systems, all obtained eigenvalues are periodically distributed in the  $\mathbf{k}$ -space along its principal directions.

### 2.3 Computation of the group velocity and evanescence criterion

The main aim of this paper is to provide a numerical methodology for optimizing the piezoelectric shunt impedance  $Z(\omega)$  for controlling energy flow into the periodically distributed acousto-piezo-composite structure. For doing this, we need to define a suitable criterion. The waves group velocities indicate how energy is transported into the considered system and allow to distinguish the 'propagative' and 'evanescent' waves. If one Bloch eigen solution (i.e  $u_n(\omega, \phi)$ ,  $k_n(\omega)$ ) is considered, the associated group velocity vector<sup>25</sup> is given by :

$$\mathbf{C}_{g_n}(\omega, \phi) = \nabla_{\mathbf{k}}\omega = \frac{\langle\langle \mathbf{S} \rangle\rangle}{\langle\langle e_{tot} \rangle\rangle} = \frac{\langle \mathbf{I} \rangle}{\langle E_{tot} \rangle} \quad (11)$$

where  $\langle\langle \cdot \rangle\rangle$  is the spatial and time average respectively on one cell and one period,  $\mathbf{S}$  is the density of energy flux defined in,<sup>25</sup>  $\mathbf{I}$  the mean intensity and  $e_{tot}$ ,  $E_{tot}$  the total piezomechanical energy and its time average on a period (see<sup>25</sup> for details). In this problem, we only consider mechanical energy transportation as the electrostatic coupling is decentralized and can be condensed as a mechanical interface as proved in<sup>26</sup> and generally computed in.<sup>27</sup> So we also compute the intensity vector  $\mathbf{I}$  by :

$$\langle \mathbf{I}_n \rangle = -\frac{\omega}{2} Re \left( \int_{\Omega} C(\varepsilon_n(\mathbf{x}, \omega, \phi) + ik\Xi_n(\mathbf{x}, \omega, \phi)) \cdot (\mathbf{w}_n^*(\mathbf{x}, \omega, \phi)) + \frac{(\nabla + ik\Phi)p_n(\mathbf{x}, \omega, \phi)p_n^*(\mathbf{x}, \omega, \phi)}{(\rho_o i\omega)} d\Omega / V_{ol} \right) \quad (12)$$

where  $*$  is the complex conjugate and  $V_{ol}$  the domain volume. As the spatio-temporal average of the system Lagrangian is null (see<sup>25</sup>), the total energy average is approximated by only computing the kinetic energy average into the solid part and acoustic energy into the fluid :

$$\langle E_{tot} \rangle = \frac{1}{2} \left( \int_{\Omega} \rho\omega^2 \mathbf{w}_n(\mathbf{x}, \omega, \phi) \cdot \mathbf{w}_n^*(\mathbf{x}, \omega, \phi) + (\rho_o C_o^2) * p_n(\mathbf{x}, \omega, \phi) \cdot p_n^*(\mathbf{x}, \omega, \phi) d\Omega / V_{ol} \right) \quad (13)$$

The group velocity vectors  $\mathbf{C}_{g_n}(\omega, \phi)$  is computed for all wave numbers at each frequency. In order to focus our analysis on only flexural modes ( $S$  and  $SH$  ones) we introduce an indicator allowing to select them by computing the ratio of kinetic energy average on out of plane displacement as:

$$Ind(n, \omega, \phi) = \frac{\frac{1}{2} \left( \int_{\Omega_x} \rho\omega^2 w_{zn}(\mathbf{x}, \omega, \phi) w_{zn}^*(\mathbf{x}, \omega, \phi) d\Omega / V_{ol} \right)}{\langle E_{tot} \rangle} \quad (14)$$

with  $w_{zn}(\mathbf{x}, \omega, \phi)$  being the ( $Oz$ ) component of vector  $\mathbf{w}_n(\mathbf{x}, \omega, \phi)$ .

### 3. OPTIMIZATION OF THE FLEXURAL MECHANICAL ENERGY FLOW AND ACOUSTIC EFFECTS

The considered piezo-composite cell is presented in figure 1. The supporting plate material is standard aluminum with 0.1 % of hysteretic damping ratio and the piezoelectric material characteristics is given in table 1. The fluid medium is made of air :  $C_o = 343 \text{ m.s}^{-1}$  and  $\rho_o = 1.25 \text{ kg.m}^{-3}$ .

The used methodology for optimizing the shunt impedance  $Z(i\omega)$  is based on the minimization of the maximal group velocity collinear to the wave number vector (11) for waves having a ratio of transported flexural kinetic energy (14) greater than 0.8. The used criterion can also be written as:

$$Crit(Z(i\omega), \phi) = \max_{n/Ind(n, \omega, \phi) > 0.8} (\mathbf{C}_{g_n}(\omega, \phi) \cdot \Phi) \quad (15)$$

The used numerical optimization of the criteria is based on a multidimensional unconstrained nonlinear minimization (Nelder-Mead).

We consider optimization by considering frequency dependent complexe impedance. We present in figure 3 the obtained real parts of the propagative wave number  $kx_n(i\omega)$  along ( $Ox$ ) axis. The red circles mark the dispersions curves for  $Z = 0$  and the blue crossed the optimal dispersion. The corresponding group velocities along ( $Ox$ ) is presented in figure 3 while the real and imaginary parts of the optimal impedance are plotted in figure 4.

| Piezoelectric Material                    |                                 |  |
|---|---------------------------------|--|
| Symbol                                    | Value                           | Property                                     |
| $s_{11}^E = s_{22}^E = s_{33}^E$          | $11.6 \times 10^{-12} Pa^{-1}$  | 11, 22 and 33 compliance matrix coefficients |
| $s_{12}^E = s_{13}^E = s_{23}^E$          | $-3.33 \times 10^{-12} Pa^{-1}$ | 12, 13 and 23 compliance matrix coefficient  |
| $s_{44}^E = s_{55}^E = s_{66}^E$          | $45.0 \times 10^{-11} Pa^{-1}$  | 44, 55 and 66 compliance matrix coefficients |
| $\eta$                                    | 0.1 %                           | Hysteretic Damping ratio                     |
| $d_{31} = d_{32}$                         | $-6 \times 10^{-11} C/N$        | 31 and 32 piezoelectric matrix coefficients  |
| $d_{33}$                                  | $15.2 \times 10^{-11} C/N$      | 33 piezoelectric matrix coefficient          |
| $d_{24} = d_{15}$                         | $730 \times 10^{-12} C/N$       | 24 and 15 piezoelectric matrix coefficients  |
| $\rho$                                    | $7600 kg/m^3$                   | Density                                      |
| $\varepsilon_{11}^T = \varepsilon_{22}^T$ | $504.1 \varepsilon_o C/V/m$     | Dielectric Permittivity                      |
| $\varepsilon_{33}^T$                      | $270 \varepsilon_o C/V/m$       | Dielectric Permittivity                      |

Table 1. Piezoelectric patch characteristics

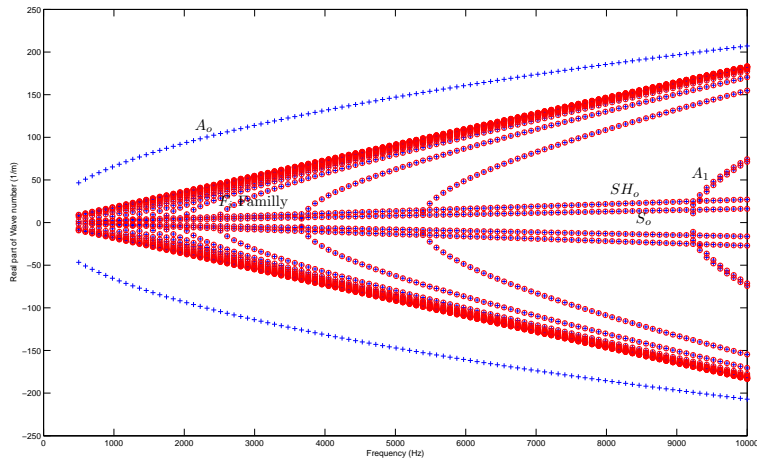


Figure 2. Real parts of the propagative wave number  $kx_n(i\omega)$  along  $(Ox)$ , the red circles mark values obtained for  $Z = 0$  and the blue crosses the optimal ones

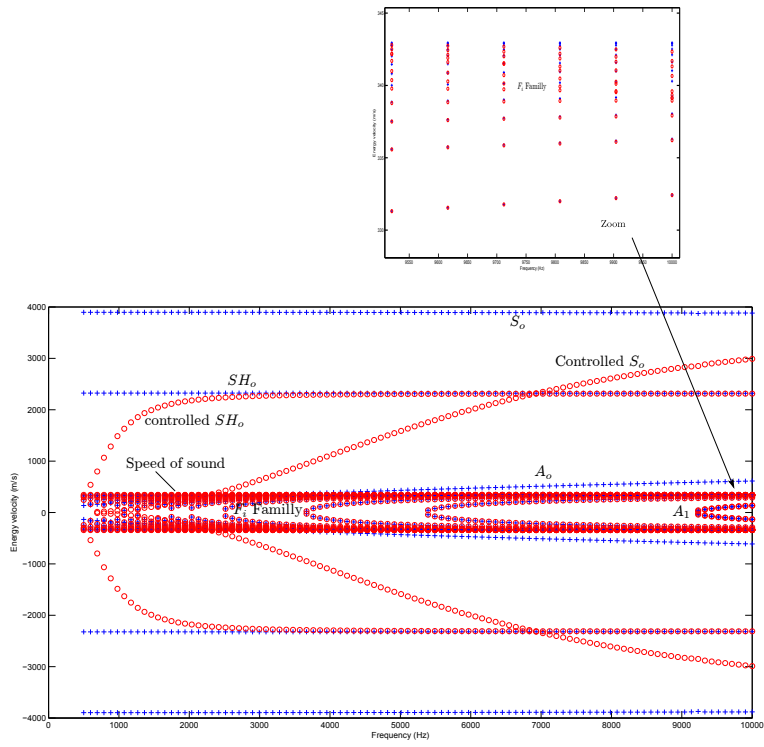


Figure 3. Group velocities along  $(Ox)$  direction; the red circles mark values obtained for  $Z = 0$  and the blue crosses the optimal ones

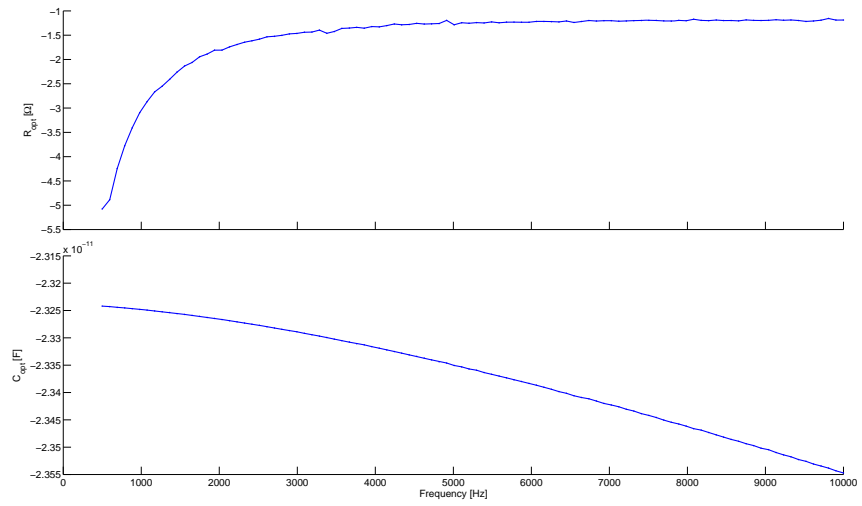


Figure 4. Real and imaginary parts of the optimal impedance

We immediately observe that the optimization of the shunt impedance leads to greatly modify the group velocity of the  $A_o$  mode and to create an evanescent mode. We notice an increase of the imaginary parts of the wave number of  $A_1$  mode indicating an increase of the spatial decay rates even if this mode remains propagative. The acoustic radiation is greatly modified by the cancellation of  $A_o$  mode as shown in figure ??c. The imaginary part of  $kz_n$  stay unchanged at very low values for radiations induced by  $A_1$ . The optimal impedance values are almost real, and correspond to those obtained if a constant negative capacitance is used. The corresponding average value is  $-233.66 \text{ pC.V}^{-1}$ . Some imaginary parts of the optimal impedance are negative,  $1.5319 \Omega$  which indicate that the optimization leads to provide energy to the system for controlling mechanical damping effect introduced with hysteretic damping ratios into the model, and, also, obtain a fully conservative system.

Acoustic wave numbers plotted on figure 3 correspond to classical dispersion on acoustic 2D tube in which the normal wave numbers  $k_z$  are ruled by the Neumann boundary condition applied on the external side of the fluidic domain. If fluid structure coupling is neglectible (i.e in laow frequency band) the normal wave numbers are  $k_{zi} = \frac{i*\pi}{L_z}$  where  $L_z = 0.5 \text{ m}$  (see figure 1). The coincidence frequency for which the in plane wave number is real clearly appears on figures 3, 3 on which we observe a family of acoustic waves denoted  $F_i$ . Control effects on acoustic waves (is quiet neglectible in the low frequency band even if some decreases on the energy velocity can be observed in high frequency on figure 3 when frequency tends to the free acoustic coincidence (here  $12.8 \text{ kHz}^{14}$ ))

#### 4. CONCLUSIONS

This paper presents a numerical procedure able to compute the wave's dispersion functions in the whole first Brillouin domain of multi dimensionnal acousto-piezo-elastodynamical wave guides. The method was applied for determining the optimal impedance allowing to minimize the group velocities of the flexural waves. The control characterisation has been done from mechanical but also acoustic point of view. We also underline a strong influence of the designed shunt circuits in the dynamical response of the mechanical system and none on the fluidic part in the tested low frequency band. We also demonstrated that our developed numerical procedures can be used for optimizing the energy diffusion operator of such adaptive mechanical interface. To do so, additional work has to be done for optimizing the complete interface scattering and for controlling the acoustic waves interacting with the mechanical system.

The proposed methodology can also be used for studying particular dissipation phenomenon such as those induced by complex shunted piezoelectric patches as proposed by<sup>7</sup> and,<sup>28</sup> or even foams or complex polymers behaviors. The proposed method furnishes an efficient tool for future optimization of distributed smart cells as proposed in the case of 1D-2D wave guide by<sup>5,14,15</sup> by extending the approach toward complex multiphysic systems.

#### ACKNOWLEDGMENTS

This work was carried out with a grant of French agency ANR number NT09–617542. We gratefully acknowledge the French ANR and CNRS for supporting this program.

#### REFERENCES

- [1] A. Preumont, *Vibration control of structures : An introduction*, Kluwer, 1997.
- [2] S. P.A. Nelson, *Active Control of Sound*, Pub. Academic Press, London, San Diego, 1992.
- [3] H. Banks and Y. W. R.C. Smith, *Smart material structures Modeling Estimation and Control*, Masson and Wiley, 1996.
- [4] H. Tzou and H. Fu, "A study of segmentation of distributed piezoelectric sensors and actuators, part i: Theoretical analysis.," *Journal of Sound and Vibration* **172(2)**, pp. 247–259, 1994.
- [5] M. Collet, K. Cunefare, and N. Ichchou, "Wave Motion Optimization in Periodically Distributed Shunted Piezocomposite Beam Structures," *Journal of Int Mat Syst and Struct* **20(7)**, pp. 787–808, 2009.
- [6] O. Thorp, M. Ruzzene, and A. Baz, "Attenuation and localization of wave propagation in rods with periodic shunted piezoelectric patches," *Proceedings of SPIE - The International Society for Optical Engineering Smart Structures and Materials* **4331**, pp. 218–238, 2001.



- [7] B. Beck, K. Cunefare, and M. Ruzzene, "Broadband vibration suppression assessment of negative impedance shunts," in *Proceedings of SMASIS08*, **6928**, ASME, 2008.
- [8] B. Beck, K. A. Cunefare, M. Ruzzene, and M. Collet, "Experimental analysis of a cantilever beam with a shunted piezoelectric periodic array," in *ASME-SMASIS*, ASME, (Philadelphia), Sept 28 Oct 1 2010.
- [9] I. Bartoli, A. Marzani, F. L. di Scalea, and E. Viola, "Modeling wave propagation in damped waveguides of arbitrary cross-section," *Journal of Sound and Vibration* **295**, pp. 685–707, AUG 22 2006.
- [10] M. Foda, A. Almajed, and M. ElMadany, "Vibration suppression of composite laminated beams using distributed piezoelectric patches," *Smart Materials and Structures* **19**(11), p. 115018, 2010.
- [11] M. S. I. S. Dawood, L. Iannucci, and E. S. Greenhalgh, "Three-dimensional static shape control analysis of composite plates using distributed piezoelectric actuators," *Smart Materials and Structures* **17**(2), p. 025002, 2008.
- [12] J. Jiang and D. Li, "Decentralized robust vibration control of smart structures with parameter uncertainties," *Journal of Intelligent Material Systems and Structures* , 2010.
- [13] B. Y. Ren, L. Wang, H. S. Tzou, and H. H. Yue, "Finite difference based vibration simulation analysis of a segmented distributed piezoelectric structronic plate system," *Smart Materials and Structures* **19**(8), p. 085024, 2010.
- [14] M. Collet, M. Ouisse, M. Ichchou, and R. Ohayon, "Smart metacomposites for semi-active control of sound radiation," in *Internoise*, (New York, USA), 2012.
- [15] M. Collet, M. Ouisse, and M. N. Ichchou, "Structural energy flow optimization through adaptive shunted piezoelectric metacomposites," *Journal of Intelligent Material Systems and Structures* **1045389X12449915**, 2012.
- [16] T. Toffoli and N. Margolus, "Programmable matter: Concepts and realization," *Physica D: Nonlinear Phenomena* **47**(1-2), pp. 263 – 272, 1991.
- [17] M. Collet, M. Ouisse, M. N. Ichchou, and R. Ohayon, "Semi-active optimization of 2D wave dispersion into shunted piezo-composite systems for controlling acoustic interaction," *Smart Materials and Structures* **21**(9), p. 094002, 2012.
- [18] G. Floquet, "Sur les équations différentielles linéaires à coefficients périodiques," *Annales de l'Ecole Normale Supérieure* **12**, pp. 47–88, 1883.
- [19] F. Bloch, "Über die Quantenmechanik der Electron in Kristallgittern," *Zeitschrift für Physik* **52**, pp. 550–600, 1928.
- [20] M. Collet, M. Ouisse, M. Ichchou, and M. Ruzzene, "Numerical tools for semi-active optimization of 2d waves dispersion into mechanical system," in *ASME-SMASIS*, ASME, (Philadelphia), Sept 28 Oct 1 2010.
- [21] G. Allaire and C. Congas, "Bloch waves homogenization and spectral asymptotic analysis," *Journal de Mathématiques Pures et Appliquées* **77**, pp. 153–208, 1998.
- [22] M. N. Ichchou, S. Akrouf, and J. Mencik, "Guided waves group and energy velocities via finite elements," *Journal of Sound and Vibration* **305**(4-5), pp. 931–944, 2007.
- [23] L. Houillon, M. Ichchou, and L. Jezequel, "Wave motion in thin-walled structures," *Journal of Sound and Vibration* **281**(3-5), pp. 483–507, 2005.
- [24] J. Mencik and M. Ichchou, "Multi-mode propagation and diffusion in structures through finite elements," *European Journal of Mechanics A-Solids* **24**(5), pp. 877–898, 2005.
- [25] W. Maysenhölder, *Körperschall-energie Grundlagen zur Berechnung von Energiedichten und Intensitäten*, Wissenschaftliche Verlagsgesellschaft, Stuttgart, 1994.
- [26] N. W. Hagood and A. H. von Flotow, "Damping of structural vibrations with piezoelectric materials and passive electrical networks," *Journal of Sound and Vibration* **146**(2), pp. 243–268, 1991.
- [27] M. Collet and K. Cunefare, "Modal Synthesis and Dynamical Condensation Methods for Accurate Piezoelectric Systems Impedance Computation," *Journal of Int Mat Syst and Struct* **19**(11), pp. 1251–1271, 2008.
- [28] F. Casadei, M. Ruzzene, B. Beck, and K. Cunefare, "Vibration control of plates featuring periodic arrays of hybrid shunted piezoelectric patches," in *Proceedings of SPIE - Smart Structures and Materials*, **7288**, SPIE, 2009.